Alqalam Journal of Medical and Applied Sciences. 2026;9(8):2535-2546
https://doi.org/10.54361/ajmas.269829

Research article

Removal of Mercury (II) Ions from Aqueous Solutions Using the Mediterranean Seagrass: Posidonia Oceanica

Labib Awin[1]*, Rabia Bennis[1], Ramadan Hadoud[2], Mahmoud El-Rais[1], Hajer Elnuri[1], Wedad Alakrash[3]

[1]*Department of Chemistry, Faculty of Science, University of Tripoli, Tripoli, Libya*
[2]*Department of Toxicology, Faculty of Medicine, University of Tripoli, Tripoli, Libya*
[3]*Plasma Research Authority for Science Research, University of Tripoli, Tripoli, Libya*
Corresponding Email. *L.Awin@uot.edu.ly*

Abstract
This work investigated the adsorption properties of *Posidonia oceanica* (P.O) with the aim of removing mercury ions from aqueous solutions. The effects of several parameters, including contact time, temperature, pH, adsorbent dose, and initial concentration, on mercury removal efficiency were determined. The thermal gravimetric analysis displayed that the (P.O) powder contains (8.96%) moisture and (2.88%) ash. The batch mode study illustrated that mercury ion removal reached equilibrium in 90 minutes at room temperature, using 0.1 g of absorbent and 25 mL of mercury solution (50 ppb, pH 2). The increase in temperature and pH resulted in lower removal percentage, whereas the increase in ionic strength resulted in higher removal capacity. The activation and enthalpy energies of the reaction were found to be - 0.32 and - 85.20 kJ/ mole respectively, where the maximum monolayer capacity of mercury adsorption was determined to be 3.37 mg/g. The isotherm and kinetic studies showed the reaction agrees with Langmuir and pseudo-second-order models (R^2 = 0.99).
Keywords. Removal Efficiency, *Posidonia Oceanica*, Mercury.

Introduction

Mercury, as a toxic heavy metal, is classified into elemental, inorganic, and organic forms. It is ranked as the sixth toxic chemical on the hazardous compounds list and is considered one of the most dangerous heavy metals in aqueous environments [1]. High mercury exposure can cause neurological issues, liver and kidney damage, and illness. Globally, Hg (II) poisoning occurs due to fish and shellfish consumption, necessitating environmental protection measures. Industries such as plastic industries, oil refineries, pulp industries, cement industries, and various other industries are also sources of mercury in the environment. In addition, mercury cells and fluorescent lamps can also become sources of mercury after usage [2]. Decontaminating or recovering mercury present in the glass, phosphor powder, and end caps of spent fluorescent lamps can become a source of mercury in the environment, Fossil fuel combustion releases 3000 tons of mercury into the atmosphere, while natural weathering processes and submarine volcanism release about 5000 tons into the ocean, the maximum allowable concentration of Hg (II) ion by world health organization (WHO) in wastewater and potable water is 5 and 1 µg/L, respectively [3].

Various methods such as ion exchange, filtration, chemical precipitation, and flotation are proposed for mercury removal, but their feasibility and cost must be considered. High operating and maintenance expenses, toxic sludge production, effluent creation, chemical consumption, mercury reuse incapacity, and the complexity of multi-step processes are the typical drawbacks of the majority of current technologies. The adsorption technique has several advantages over other techniques, including design simplicity, ease of operation, and high removal efficiency, which could reach (90–99%) [4]. It has shown positive results in sequestering heavy metals. It is a potentially effective alternative to traditional treatment processes for metal ion removal. It is a technically feasible and economically viable sustainable technology for the treatment of wastewater streams [5].

Biosorption is a technique based on a property of certain types of inactive, dead biomass to bind and concentrate heavy metals from even very dilute aqueous solutions. It appears as a complex phenomenon where the metallic species could be deposited in the solid biosorbent through different sorption processes of ion exchange, complexation, chelation, and precipitation [6]. Several adsorbents were produced and utilized from agriculture and industries such as seagrasses, molds, yeast, bacteria, crabshells, wool, rice, straw, peat moss, tea leaves, and coconut fibre. The role of dried seagrass in the removal of toxic metal ions from water has attracted great attention due to its high area-to-volume ratio that provides a large contact area for metal binding. The ability of such substances to adsorb metals depends on various factors such as the bioavailability of metals and their uptake capacity. The uptake of metals in adsorbents depends on the surface reaction in which metals are absorbed through electrostatic attraction to negative sites. For instance, metal cations with high electronegativity and small ionic radii are preferably absorbed by algae biomass. The metal accumulation capacity of biomass is sometimes higher than that of chemical sorbents [7]. An example of seagrass is *Posidonia oceanica,* which is an endemic marine magnoliophyte found in the Mediterranean Sea. It forms large underwater meadows from the surface to depths of 40 m, which are an important part of the ecosystem. The seagrass forms structures known as mats, which are monumental constructions that result from the horizontal and vertical growth of the rhizomes with their entangled roots and the entrapped sediment. The fibers accumulate in considerable quantities, reaching a thickness of 1–2 m or more on the most Mediterranean beaches [8]. This seagrass is very sensitive to human disturbance, such as coastal development, pollution, trawling, and high-water turbidity. Huge quantities of these wastes

Received: *10-06-2026 -* ***Accepted:*** *08-08-2026 -* ***Published:*** *17-08-2026*

are either transported (or possibly buried) in landfills, or piled up in adjacent areas to beaches or even re-immersed in the sea. In this study, the removal of Hg^{2+} from aqueous solutions using *Posidonia oceanica* is presented. The effect of contact time, pH, adsorbent mas and temperature was studied for that metal sorption procedure, as well as heavy metal equilibrium sorption kinetics.

Experimental

Sample preparation

The P.O grass (a flowering plant that lives in dense meadows) was collected along north Western coast of Libya (Tajora). The leaves are ribbon-like, bright green, turning brown with age. The biosorbent was prepared from the leaves, after being rinsed with tap water to remove impurities such as sand and salt absorbed at the surface of the biomass. Then it was washed with distilled water and dried at room temperature for 7 days. The dried sample was ground to a fine powder in mill and sieved to get a size fraction (150 micron). The stock solutions of Hg^{2+} ions with a concentration (50 ppb) were prepared by diluting analytical grade solution (1000 ppm) with distilled water. The initial pH was adjusted to the desired value using value using 0.1 N HCl or NaOH.

Instrumentations

The P.O powder was characterized using Fourier transform infrared spectroscopy (FTIR) and a scanning electron microscope (SEM). The (FTIR) spectroscopy was used to give a qualitative analysis of the main chemical groups present on the sample and responsible for the adsorption. The translucent sample of disks were prepared by mixing the P.O powder with KBr; the spectra were recorded with a PerkinElmer Spectrum Two. The purpose of using scanning electron microscopy (SEM, JEOL JSM – 561OLV) is to provide a view of the morphological structure. The moisture and ash percentages in the P.O samples were determined using thermal gravimetric analysis. The concentrations of mercury (II ions in solutions were estimated by a mercury analyzer (LabAnalyzer 245) located at the toxicology department in the University of Tripoli. The pH measurements were carried out on a WTW720 pH meter model CT16 2AA (LTD Dover Kent, UK) and equipped with a combined glass electrode.

Batch mode

Batch mode removal studies were carried out by varying several parameters such as contact time, pH, temperature and mass of adsorbent. Essentially, a 50 ml of stock solution with a concentration of 50 ppb was taken in a 250 ml conical flask in which the initial pH was adjusted using HCl/NaOH. Optimized amount of adsorbent was added to the solution and stirred using a magnetic stirrer for a specific time. The P.O samples were separated from the solutions using a centrifuge (4500 CPM for 5 minutes).

Result and Discussions

Characterization of P.O grass

The morphology plays an important role in the adsorption and removal of Hg (II) on the external surface. A scanning electron microscope image for P.O powder is presented in (Figure 1). The P.O sample exhibits a well-defined lignocellulosic fibrous structure with cylindrical fiber shapes, which is favourable for metal ions adsorption. Compared to a smooth-surface material, the surface shape of P.O provides an advantageous area for ions uptake due to the material's outer layers that can facilitate the solute's diffusion to the centre of the particles.

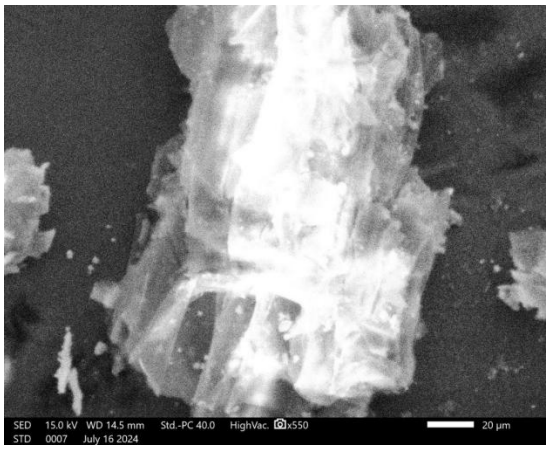

Figure 1. A scanning electron microscope image for P.O powder.

FT-IR spectra for P.O were recorded before and after Hg (II) adsorption (Figure 2). The first part of the spectra (in the range 4000–2000 cm^{-1}) is poorly resolved: **(a)** a broad band is observed in the range 3700–3000 cm^{-1}, which is representative of the convolution of the signals for different vibration modes such as free OH, O–H stretch, and inter-chains H-bonds, **(b)**

Received*: 10-06-2026 -* ***Accepted****: 08-08-2026 -* ***Published****: 17-08-2026*

two small peaks are recorded at 2919 $cm^{-1}$and 2855 cm^{-1} that correspond to symmetric –CH_2 valence vibration and –CH stretching vibration respectively. It is generally difficult finding useful information from this wavenumber range and spectrum analysis is generally focused on the 2000–600 cm^{-1} region, A band is observed close to 1652cm^{-1}this band is attributed to C = O stretch, conjugated p-substituted aryl ketones. On this broad band, a shoulder can be observed at 1728 cm^{-1}, this is representative of either C = O stretch in unconjugated ketones, carbonyls and in ester groups (especially in carbohydrates) conjugated aldehydes and carboxylic acids, or C = O valence vibration of acetyl or COOH groups, The peak at 1534 cm^{-1} can be identified in amine/amide groups and in carboxyl groups. A series of peaks are identified in the range 1430–1300 cm^{-1}, they are non-specific bands that readily identified in cellulose material (1423, 1371, 1314 cm^{-1}) because the biopolymer is more crystalline than other constituents of hemicelluloses and lignin. Another broad band appears at $1241cm^{-1}$ that was attributed to symmetric stretching in carboxyl groups, that was attributed to symmetric stretching in carboxyl groups, The broad band around 1100 cm^{-1} (with a series of small peaks) is representative of carbohydrate ring bonds. The peak at 891 cm^{-1}can be probably attributed to anomere C-groups and ring valence vibration. Similar results were previously reported by Ashour (2021) [9] and Allouche (2024) [10]. After Hg (II) binding, the spectrum is not drastically modified. The main differences can be observed: (**a**) in the range 1750–1600 cm^{-1} where the width of the broad band is reduced (sharper and more resolved peak); (**b**) at 1534 cm^{-1} where the shoulder was less marked; (**c**) at 1423 $cm^{-1}$and 1371 $cm,^{-1}$where the peaks slightly decreased. This probably means that some amine/amide groups may be involved together with cellulose functional groups. The band representative of the aromatic skeletal vibration of the phenol and phenolate in lignin are supposed to appear around (1495-1512 cm^{-1}) respectively, they may contribute in the change of the bands in this wavenumber range after metal sorption through the probable contribution of phenolic compounds.

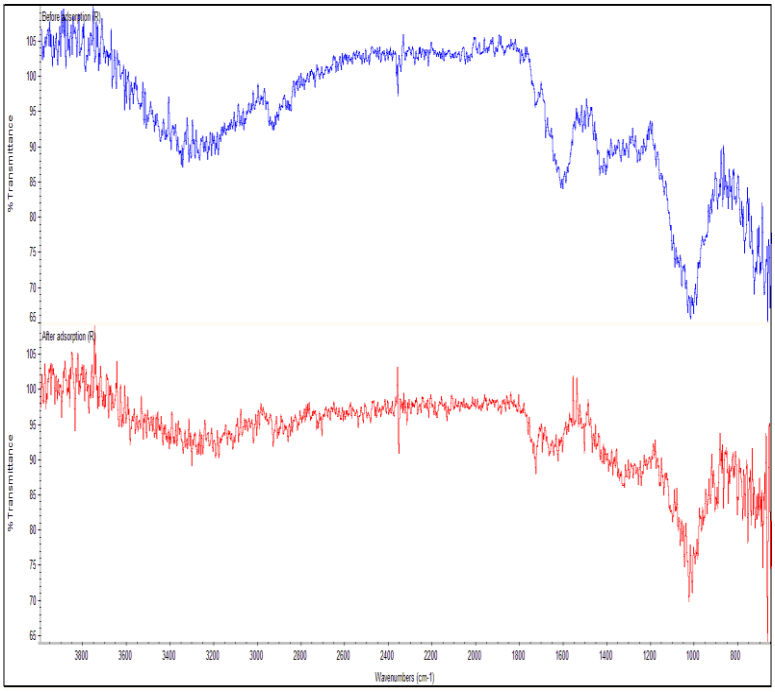

Figure 2. FTIR spectra of Posidonia oceanica before and after Hg (II) adsorption.

The P.O sample was thermally gravimetrically analysed by drying 1.0 g of the grass in the oven at 250 C° for 48 hours and burning 1.0 g at 600 C° for 2 hours. The analysis result displayed that the (P.O) powder contains (8.96%) moisture and (2.88%) ash.

Batch Mode Results

Effect of Contact Time

Understanding the kinetics of mercury removal using P.O grasses possibly aids in addressing pollution issues in marine and coastal ecosystems. Researchers can assess these plants' efficacy as natural filters in contaminated streams by observing how long it takes to absorb mercury ions, leading to more effective environmental regulations and enforcement mechanisms. The removal percentage of Hg^{2+} over the absorbent can be calculated as: $R\% = [(C_i-C_t)/C_i] \times 100$ [11], where R% is the removal percentage, C_i = 50 ppb is the initial concentration of mercury solution, C_t is the concentration of Hg^{2+} ions at contact time estimated from the concentration dependence of absorbance fit. The effect of contact time was investigated in the range of 0 to 120 min using 0.1 g of P.O. The equilibrium point of adsorption (99.90%, 0.0125 mg/g) was observed within 90 min.

Received: *10-06-2026 -* ***Accepted:*** *08-08-2026 -* ***Published:*** *17-08-2026*

https://doi.org/10.54361/ajmas.269829

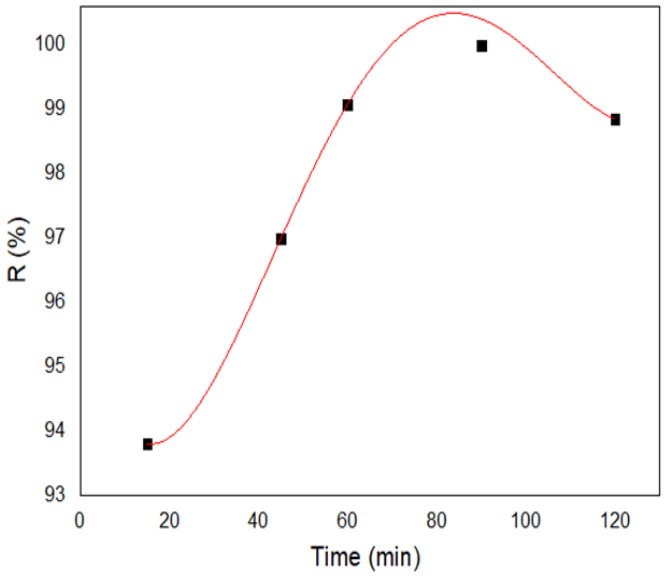

Figure 3. Time dependence of removal percentage using 0.1 g of P.O. The volume, concentration and pH of the mercury solution are 25 ml, 50 ppb and 2 respectively. The red line in the figure is the polynomial fitting of the experimental data, which is expressed as: R % =95.82- 0.28 t+1.30×$10^{-2}t^2$-1.28×10^{-4} t^3+4.29×$10^{-7}t^4$(R^2 = 0.95).

As seen in (Figure 3), the process of biosorption was high at the initial stage and became slower while approaching the equilibrium stage at 90 min. This is obvious due to the fact that a greater number of vacant negatively charged sites are available initially on the surface of the biosorbent, and the sites are gradually filled up while approaching equilibrium and are filled completely at equilibrium [12]. These results agree with previous studies conducted by Dou (2011) [13], which demonstrated that the maximum adsorption rates (98.60%) of mercury are determined within the first 45 minutes using TiO_2 nanoparticles, and also agree with the study of Hardani (2015) [14] in which the adsorption reaches equilibrium at approximately 10 minutes due to the high adsorption capacity of Fe_3o_4 /HAP for mercury (492.2 mg/g).

Effect of pH

This parameter directly influences the surface charge of the adsorbent and the ionization of the adsorbate. It also affects the adsorption efficiency either positively or negatively [15]. Understanding the relationship between pH and adsorption leads to enhanced water purification techniques, especially in removing contaminants like heavy metals and harmful organic compounds. In this work, the effect of pH was evaluated in the range of (2 to 9). The removal percentage of Hg^{2+} ions as a function of pH is shown in (Figure 4). The adsorption amount escalates dramatically at pH values higher than 6. This is attributed to the fact that adsorption leads to the reduction of the metal concentration in the basic solutions. pH affects both the metal ion speciation and the ionization state of the P.O surface functional groups. At strongly acidic conditions, surface functional groups are protonated; thus, the approach of positively charged species is inhibited. As pH increases, the negative charge density on the P.O surface increases due to deprotonation of active sites, and therefore the approach of positively charged ions is promoted. At lower pH, such as 4.5, mercury exists mostly in the form of $HgCl_2$ but when the pH of the solution increases, the solubility of mercury decreases due to extensive hydrolysis as HgClOH and Hg $(OH)_2$ species [15]. Hence, the P.O sorption capacity increases to a certain limit depending on the mercury fraction remaining in solution. These results are correlated with previous studies conducted by Hardani (2015) [14] which investigated the relationship between the initial pH values and the quantities of Hg^{+2} ions adsorbed by 50 mg of $Fe_3\,O_4$/HAP at 25 C^0(initial concentration 25 ng/ml). Hardani found that the Hg ions uptake experiences continuous increase by raising the pH value, moreover, the adsorption amount escalates dramatically in pH range higher than 7.

Received: *10-06-2026 -* ***Accepted:*** *08-08-2026 -* ***Published:*** *17-08-2026*

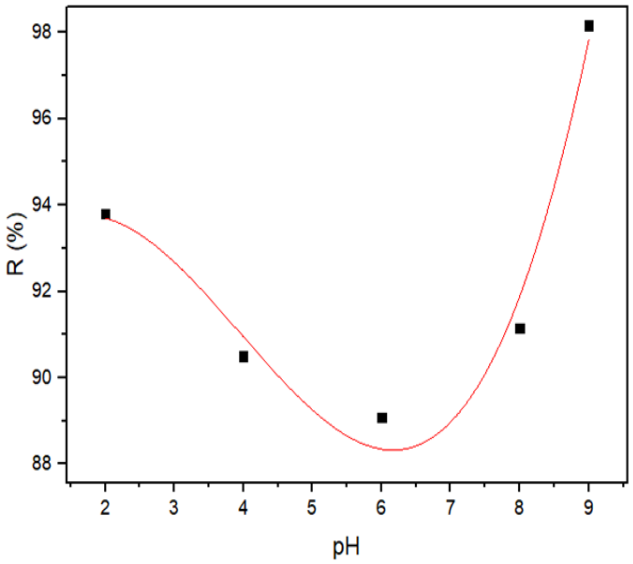

Figure 4. Removal percentage of mercury ions as a function of pH using 0.1 g of P.O. The volume, concentration, and temperature of the mercury solution are 25 ml, 50 ppb, and 25 °C, where the contact time is 30 minutes. The red line in the figure is the polynomial fitting of the data which is expressed as: $R\% = 90.59 + 4.00x - 1.48x^2 + 0.12x^3$ ($R^2 = 0.97$), ***where x is the value of pH.***

Effect of Adsorbent dose

The quantity of adsorbent required for a recovery of particular chemicals can be optimized by figuring out how different masses of adsorbent affect the adsorption capacity. The production and application of adsorption techniques in a variety of sectors can be made less expensive by determining the ideal mass of adsorbent for a particular purpose. Investigating this relationship advances our basic knowledge of surface chemistry and the mechanisms underlying interactions between the adsorbent and adsorbed. The effect of biosorbent dose on Hg^{+2} removal was investigated using a mass range of 0.1 g to 0.5 g, where other parameters like pH, Initial concentration, and contact time were optimized at pH 2, 50 ppb, and 30 min, respectively. The amount of the Hg^{+2} adsorbed by one gram of the P.O grass (q) was calculated as following: q (mg/g) = $[(C_i-C_t)\times V]/W$ [11], where t is the contact time, V= 25 ml is the volume of Hg^{2+} ions solution and W is the mass of P.O. The relationships between adsorbent mass versus removal percentage and inverse capacity (1/q) are illustrated in (Figure 5).

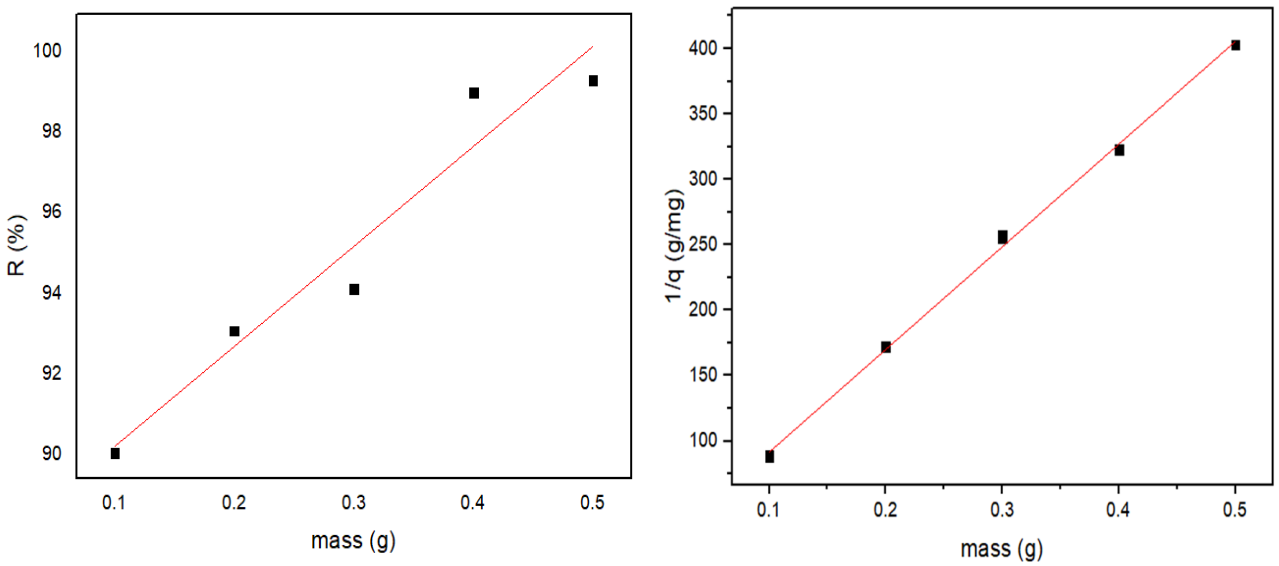

(a) **(b)**

Figure 5. (a) Adsorbent dose versus Removal and (b) Adsorbent dose versus inverse capacity. The volume, concentration, and temperature of the mercury solution are 25 ml, 50 ppb, and 25 °C, where the contact time is 30 minutes. The red line in the figure is the linear fitting of the data. The correlation between mass dose (m) and inverse capacity (1/q) can be expressed as $1/q=12.95+7.85\times10^2 m$ ($R^2 = 0.99$)

Received: *10-06-2026 -* ***Accepted:*** *08-08-2026 -* ***Published:*** *17-08-2026*

Increasing the biosorbent dose provides greater surface area and availability of more active sites, thus leading to the enhancement of mercury ion uptake. As shown in (Figure 5), the removal percentage increased from 89.58 to 99.29% as the biosorbent dose increased from 0.1 to 0.5 g. Correspondingly, the removal capacity decreased from (1.12×10^{-2} mg/g) to (2.50×10^{-3} mg/g). The maximum experimental capacity (q_{exp}) can be calculated from the linear fitting equation of the correlation between inverse removal capacity and adsorbent mass. The value of q_{exp} was calculated to be 77.2×10^{-2} (mg/g) when the mass is zero. This amount is much lower than those reported [16] for the divalent metal ions Pb (48.3 mg/g), Cu (43.9 mg/g), Ni (41.0 mg/g), Zn (37.9 mg/g), and Cd (30.2 mg/g) adsorbed by P.O at pH 6.

Effect of Temperature

Finding the relationship between temperature and adsorption is crucial for various fields, including chemical engineering, environmental science, material science, and biotechnology. It aids in optimizing adsorption procedures, enhancing remedial techniques, and improving the performance of adsorbents in various applications. To assess the effect of temperature on adsorption, experiments were conducted at various temperatures 35^0, 40^0, 45^0, 50^0, 55^0 and 60^0C. As presented in (Figure 6), the removal percentage decreases as the temperature increases, reflecting the exothermic nature of mercury adsorption on *the Posidonia oceanica* surface. This result is consistent with earlier research by Dou et al. (2011) [13], which showed the largest adsorption rates of mercury on titanium dioxide are obtained at the temperature of 22^0 C and the adsorption decreases as temperature increases.

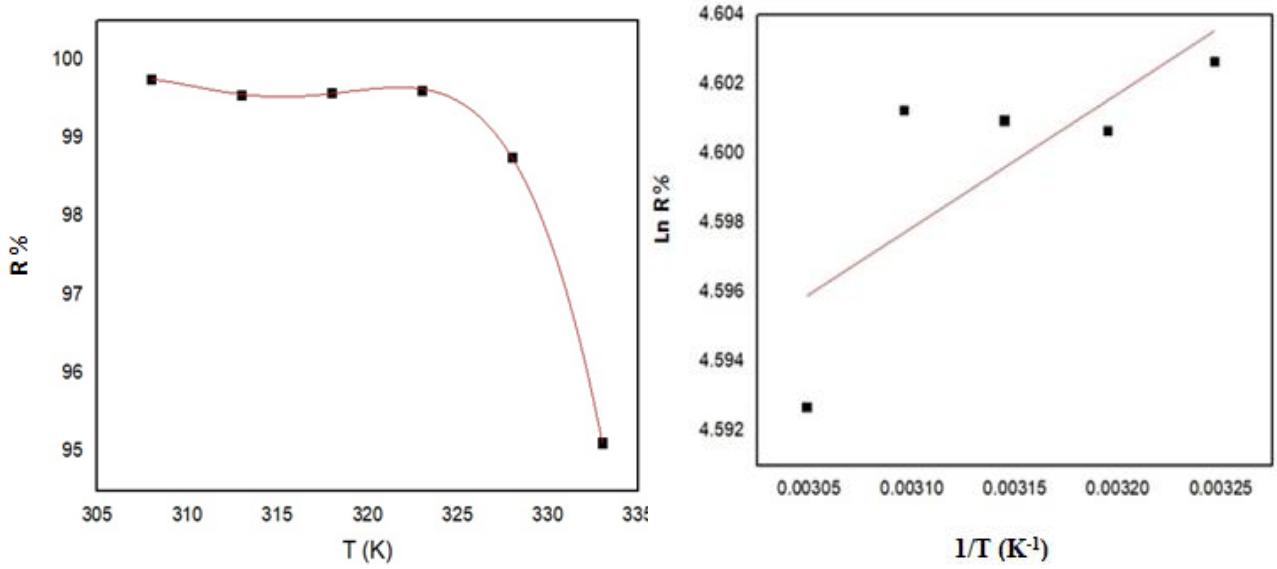

(a) **(b)**

Figure 6. ***(a) Temperature dependence of removal, and (b) Arrhenius plot of removal. The volume, concentration, and pH of the mercury solution are 25 mL, 50 ppb, and 2, where the contact time and P.O mass are 30 minutes and 0.1 g. The red lines on the left and right-hand side figures are the polynomial and linear fitting of the data. The correlation between removal percentage and temperature can be expressed as*** $R\% = 6.97\times10^3T - 33.23\,T^2 + 0.07T^3 - 5.59\times10^{-5}T^4 - 5.47\times10^5$ $(R^2 = 0.99)$

The modified formula of the Arrhenius equation: $\ln R\% = \ln R_0\,\% - E_a/RT$ [17]; can be used to determine the activation energy of the reaction, where R_o % is the value of initial removal, E_a is activation energy (J/mol), T is temperature (K), and R is general constant of gases. The plot of ln R% versus 1/T gives values of intercept and slope equal to 4.48 and 38.67, respectively. The activation energy as estimated from the slope was found to be - 0.32 kJ/mol. This value is relatively lower compared to the energy associated with physisorption, indicating that physical interactions may be a part of the adsorption process.

Effect of Ion Strength

The electrostatic interaction is known as an important factor that drives forces for pollutant adsorption in aqueous solutions. Such a factor can be controlled by maintaining the ion strength of the solutions, which has an ambiguous impact on the adsorption process. Here, the ion strength effect on mercury removal was investigated by adding gradual amounts of 0.05, 0.1, 0.15, and 0.2 g of NaCl to the solutions. (Figure 7) shows that the removal of mercury ions increases as the amount of NaCl increased. This means the electrostatic interaction between mercury ions and the sea grass was enhanced by increasing the ion strength of the solutions. The theory behind such behavior stems from the role of the electrical double layer on the wettability of amphoteric surfaces. The salt concentration influences the diffuse part of the electrical double layer, which in turn affects the surface charge and thereby the surface wettability [18]. A quantitative understanding of such an impact on the surface energy of amphoteric solids is still missing.

Received: *10-06-2026 -* ***Accepted:*** *08-08-2026 -* ***Published:*** *17-08-2026*

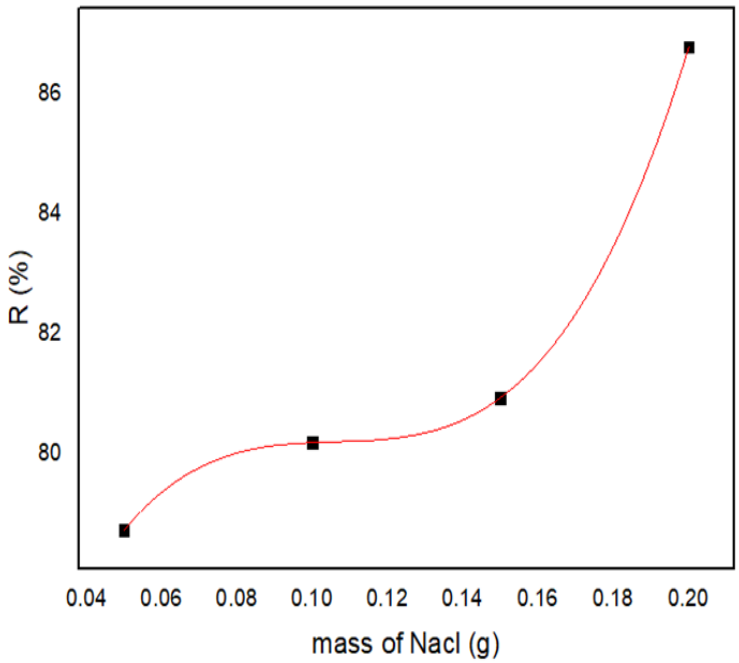

Figure 7. The Impact of Ion Strength on Mercury Removal. The volume, concentration, and pH of the mercury solution are 25 mL, 50 ppb, and 2, where the contact time and P.O mass are 30 minutes and 0.1 g. The red lines in the figure are the polynomial fitting of the data. The relationship between mercury removal (R%) and the mass of NaCl (x in g) can be expressed as: $R\% = 70.75 + 2.64 \times 10^2 x - 2.46 \times 10^3 x^2 + 7.75 \times 10^3\ x^3\ \ (R^2 = 0.99)$.

Effect of initial concentration

One element that may influence adsorption is the initial concentration of adsorbate. As illustrated in (Figure 8), the increase in the initial concentration of Hg (II) ions resulted in a lower removal percentage. This is due to the increase in the adsorbate amounts on the absorbent surface, which leads to a quick saturation of the adsorption sites and consequently reduces the removal percentage.

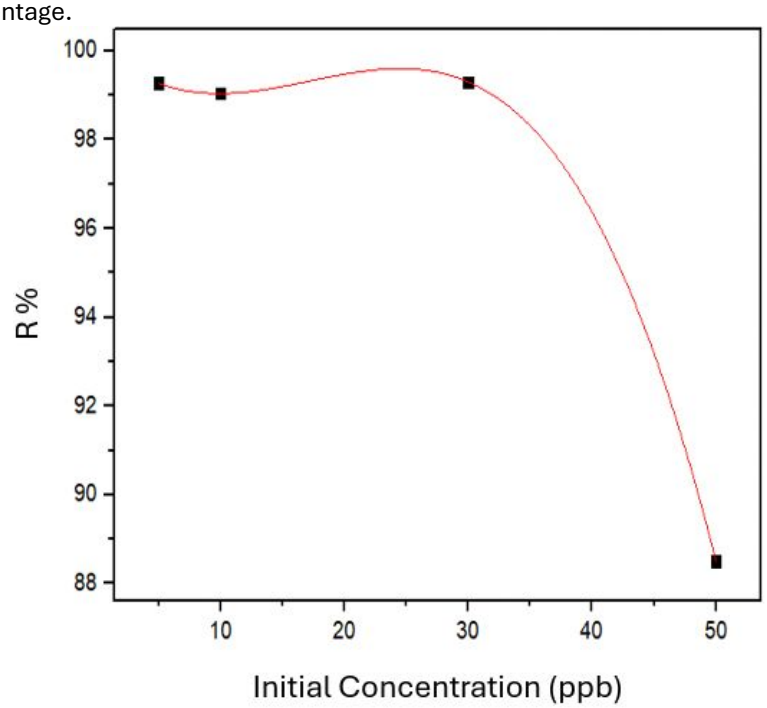

Figure 8. Initial concentration dependence of removal. The volume, temperature and pH of the mercury solution are 25 mL, 25 ° C and 2, where the contact time and P.O mass is 30 minutes and 0.1 g. The red lines in the figure is the polynomial fitting of the data that is expressed as R % =100.20 - 0.27 C_i + 1.89×$10^{-2}$$C_i^2$ + 4.00×10^{-3} C_i^3 (R^2 = 0.99).

Thermodynamic studies of mercury Adsorption

The study of the thermodynamic functions aid to anticipate the reaction's viability, which is typically the first step in investigating a reaction. The following equation: $\Delta G^0 = -RTlnK_e$ [19]; can be used to calculate standard Gibbs free energy for adsorption at a specific temperature using the thermodynamic equilibrium constant. Where ΔG^0 (kJ/mol) is

Received: *10-06-2026 -* ***Accepted:*** *08-08-2026 -* ***Published:*** *17-08-2026*

https://doi.org/10.54361/ajmas.269829

Gibbs energy, T (K) is the absolute temperature; R (kJ /mol.K) is the general gas constant; and K_e is the thermodynamic equilibrium constant. The latter can be calculated from the equation: $K_e = \frac{q_e}{C_e} \times m$ [19]; where q_e (mg/g) and C_e (ppm) are the removal capacity and remaining concentration at the equilibrium point, and m (g/L) is the mass of the adsorbent. According to the obtained results in (Table 1), the negative values of ΔG^0 reflect that the adsorption process is a spontaneous reaction based on the experimental conditions. As the temperature increases, the tendency for adsorption decreases.

Table 1. Gibbs Free Energy Versus Temperature

T (K)	ΔG^0(kJ/mol)
308	-15.39
313	-14.07
323	-14.89
328	-11.64
333	-8.54

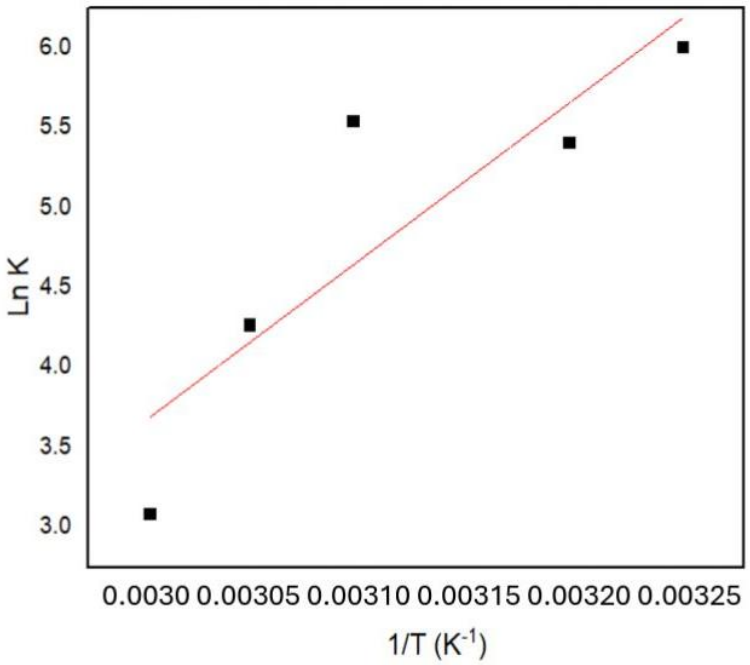

Figure 9. The Logarithm of Equilibrium Constant Versus Inverse Temperature. The volume and pH of the mercury solution are 25 ml and 2, where the contact time and P.O mass is 30 minutes and 0.1 g. The red lines in figure is the linear fitting of the data.

The standard enthalpy (ΔH^0) and entropy (ΔS^0) are defined in the following equation: $\Delta G^0 = \Delta H^0 - T\,\Delta S^0$ [19] where the logarithm of the equilibrium constant is expressed as $\ln K_e = -\frac{\Delta H^0}{R}\left(\frac{1}{T}\right) + \frac{\Delta S^0}{R}$ [19]. The standard enthalpy and entropy can be estimated from the linear plot of ln K_e versus 1/T (Figure 9). Where the slop is equal to $\frac{-\Delta H^0}{R}$ and the intercept is equal to $\frac{\Delta S^0}{R}$. Accordingly, ΔH^0 and ΔS^0 are found to be -85.20 and -0.23 kJ/mol, respectively. The negative values reflect that the adsorption of mercury on the P.O surface is typically defined as an exothermic reaction associated with reduced disorder.

Adsorption isotherms

Langmuir adsorption isotherm

The linear form of the Langmuir isotherm is given as: $\frac{C_e}{q_e} = \frac{1}{q_m k_L} + \frac{C_e}{q_m}$ [20], where q_m is the maximum monolayer capacity (mg/g), and K_L is the langmuir constant (L/g), which is related to the binding energy of the mercury ions to the active site.

Received*: 10-06-2026 -* ***Accepted****: 08-08-2026 -* ***Published****: 17-08-2026*

https://doi.org/10.54361/ajmas.269829

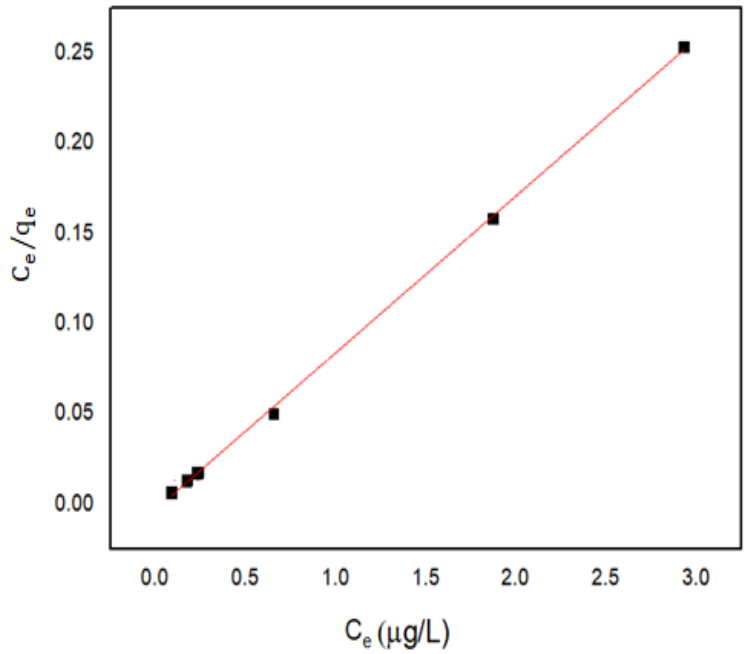

Figure 10. Langmuir isotherm of mercury removal on P.O surface. The red lines in figure is the linear fitting of the data.

The linear plot of C_e/q_e against C_e (Figure 10) illustrates that the adsorption is in good agreement with the Langmuir model ($R^2 = 0.99$). The maximum monolayer capacity q_m and the Langmuir constant K_L of the mercury adsorption were 3.37 mg/g and 0.90 L/mg respectively. The Langmuir isotherm is a valid for monolayer sorption onto a surface with a finite number of identical sites and uniform adsorption energies [20].

Freundlich adsorption isotherm

The linear form of the Freundlich Equation can be expressed as seen in the equation: $Ln\ q_e = ln\ K_f + \frac{1}{n} ln\ C_e$ [20] where q_e is the amount adsorbed at equilibrium concentration (mg/g), K_f is the empirical constant of the Freundlish isotherm (L/mg) and C_e is the equilibrium concentration of mercury ions in solution (mg/L), the constant n is the empirical parameter related to the intensity of adsorption. Fitting the data using the Freundlich adsorption isotherm (Figure 11) gives a semi-linear relationship with $R^2 = 0.78$, $K_F = 0.70$ and $1/n = 0.64$, respectively.

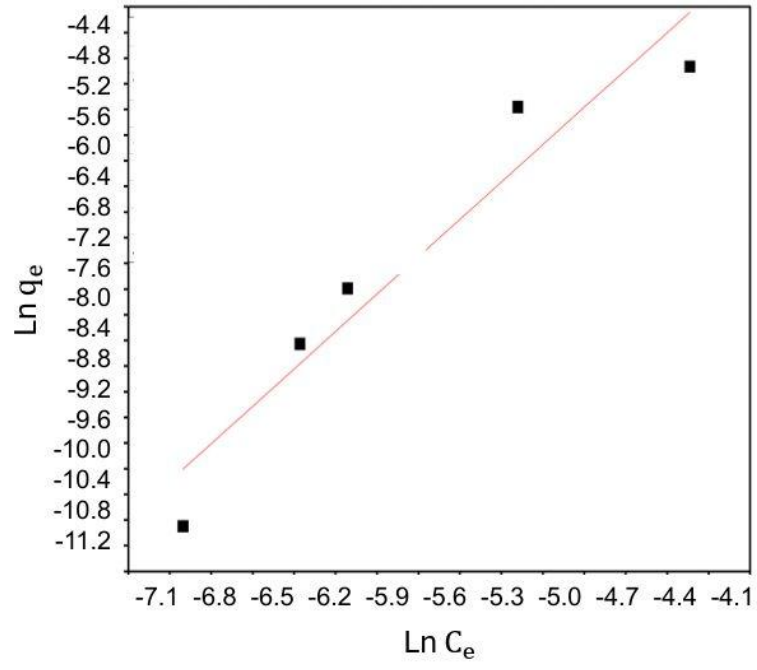

Figure 11. Freundlich isotherm of mercury removal on P.O surface. The red lines in figure is the linear fitting of the data.

Received: *10-06-2026 -* ***Accepted:*** *08-08-2026 -* ***Published:*** *17-08-2026*

https://doi.org/10.54361/ajmas.269829

Temkin adsorption isotherm

The linear form of the Temkin isotherm is expressed as: $q_e = B_1 \ln C_e + B_1 ln K_T$ [20], where $B_1 = {}^{RT}/_{b}$ is a constant, depending on the adsorption heat and K_T (L/g) is the Temkin isotherm constant, the plot q_e versus LnC_e , gives a straight line where B_1 is determined by slop (B_1) and K_T by an intercept ($B_1\ lnK_T$). (Figure 12) illustrates a linear relationship with $R^2 = 0.86$, $B_1 = 3.56$, and $K_T = 5.60$.

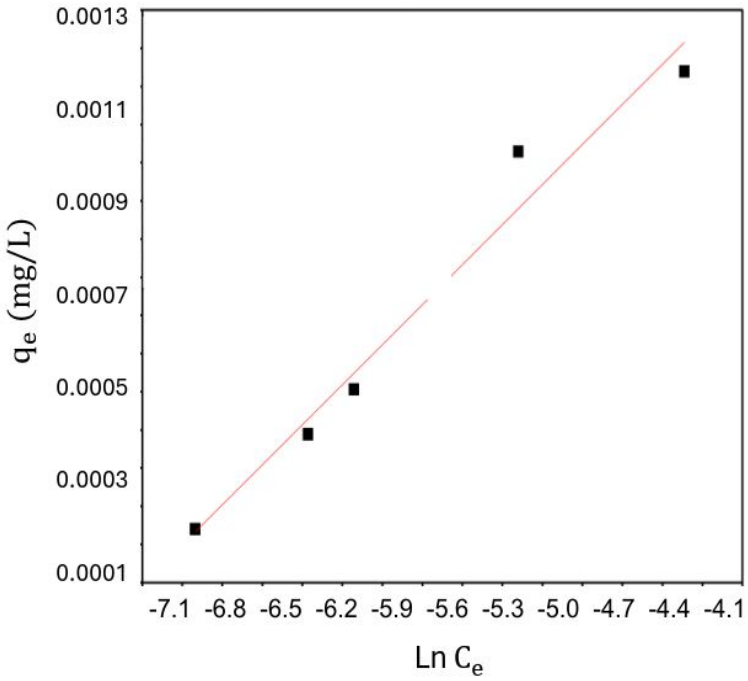

Figure 12. Temkin isotherm of mercury removal on P.O surface. The red lines in figure is the linear fitting of the data.

Adsorption Kinetics

Kinetics studies are among the most significant research on the adsorption process; they investigate the impact of contact duration on the removal rate. Lagergern's pseudo-first-order equation: $\ln(q_e - q_t) = \ln q_e - K_1 t$ [21] serve as the basis for the adsorption kinetics models, where k_1 (/h) is the Lagergern rate constant, q_e and q_t are the amounts of mercury ions adsorbed per unit mass of the adsorbent at equilibrium and t is time. The plot of ln ($q_e - q_t$) versus t (Figure 13) shows no straight line, which reflects that the kinetics of the mercury removal reaction by *posidonia oceanica* does not agree with the pseudo-first-order model.

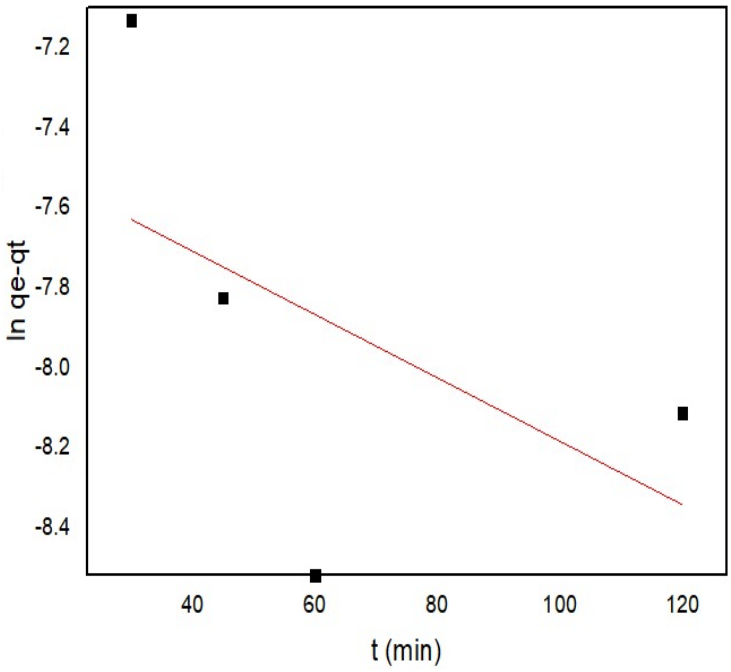

Figure 13. Pseudo-first-order model of mercury removal on P.O surface. The red line in figure is the linear fitting of the data.

Received: *10-06-2026 -* ***Accepted:*** *08-08-2026 -* ***Published:*** *17-08-2026*

https://doi.org/10.54361/ajmas.269829

The pseudo-second order mechanism by Ho et al. [21] is presented in the equation: $\frac{t}{q_t} = \frac{1}{{q_e}^2 k_2} + \frac{1}{q_e}$ t. Where K_2 is a constant rate for a pseudo-second order equation, which is obtained from the plot of t/q_t versus t (min) (Figure 14). The fitting of this relationship was found to be linear (R^2=0.99), which means that the kinetic of the mercury removal reaction agrees with pseudo-second order model. The K_2 and q_e Can be calculated using the straight line fitting where $\frac{1}{q_t}$ is the slope and $\frac{1}{{q_e}^2 k_2}$ is the intercept. The values of K_2 and q_e are found to be 75.53 (g/mg. min) and 0.12 mg/g, respectively. Comparing the correlation factors of the adsorption isotherms and kinetics, it can see that pseudo- second order model presented the highest correlation factor (R^2= 0.99) whereas pseudo- first order model showed the lowest correlation (R^2= 0.29).

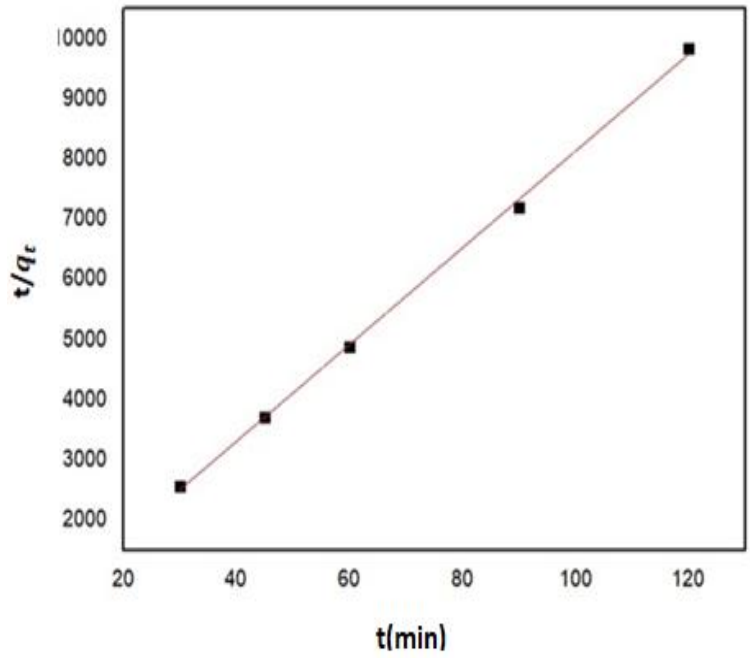

Figure 14. Pseudo-second order model of mercury removal on P.O surface. The red line in figure is the linear fitting of the data.

Conclusion

To conclude, *posidonia oceanica* showed good properties as a natural filter for mercury in aqueous solutions. This was evident by scanning electron microscopy, which showed that P.O grass has a rough surface that aids to uptake of mercury by friction. Also, IR measurements showed P.O has several active functional groups for mercury adsorption, as illustrated by changes in the ranges of 1750–1600 cm^{-1} and 1423- 1371 $cm,^{-1}$ before and after the adsorption. The thermal gravimetric analysis displayed the humidity percentage of P.O is 8.96% where the ash percentage is 2.88%. The batch mode study stated the optimum conditions for Hg (II) ion removal on P.O surface are: contact time= 90 min; adsorbent dosage= 0.1 g; initial concentration of Hg (II) ions= 50 µg/L; temperature=35°C, and pH= 2. In addition, the maximum adsorption capacity q_m of Hg (II) ions was estimated to be 3.37 mg/g. The activation energy as calculated from the Arrhenius equation is - 0.32 kJ/mole. The thermodynamic functions: ΔH^0 and ΔS^0 are found to be -85.20 and -0.23 kJ/mol, respectively. The isotherm models showed that the kinetics of mercury removal are strongly correlated with the Langmuir isotherm model and the second- pseudo equation, but the correlation was weaker with Freundlich and Temkin models.

Conflicts of Interest

The authors declare no conflicts of interest.

Acknowledgment

The authors thank Plasma Research Authority for its assistance in FTIR measurements.

References

1. Al-Ghouti MA, Da'ana D, Abu-Dieyeh M, Khraisheh M. Adsorptive removal of mercury from water by adsorbents derived from date pits. Sci Rep. 2019;9(1):15327.
2. Agarwal SK. Water pollution. New Delhi: A.P.H. Publishing Corporation; 2005.
3. Mistar EM, Hasmita I, Alfatah T, Muslim A, Supardan MD. Adsorption of mercury(II) using activated carbon produced from Bambusa vulgaris var. striata in a fixed bed column. Sains Malays. 2019;48(4):719–725.

Received*: 10-06-2026 -* ***Accepted****: 08-08-2026 -* ***Published****: 17-08-2026*

4. Rouquerol F, Rouquerol J, Sing KSW. Adsorption by metal oxides (Chapter 10). In: Rouquerol F, Rouquerol J, Sing KSW, editors. Adsorption by powders and porous solids: principles, methodology and applications. London: Academic Press; 1999. p. 287–354.
5. Raji Z, Karim A. Adsorption of heavy metals: mechanisms, kinetics and applications of various adsorbents in wastewater remediation (a review). Waste. 2023;1(3):775–805.
6. Abdel-Ghani NT, El-Chaghaby GA. Biosorption for metal ions removal from aqueous solutions: a review of recent studies. Int J Latest Res Sci Technol. 2014;3(1):24–42.
7. Biswal BK, Balasubramanian R. Use of biochar as a low-cost adsorbent for removal of heavy metals from water and wastewater. J Environ Chem Eng. 2023;11(5):110986.
8. Augier H, Eugene C, Hamand J, Sougy A. Posidonia oceanica re-implantation technology of the marine gardeners is now operational on a large scale. Ocean Coast Manag. 1996;30(2-3):297–307.
9. Ashor HM, Awin LA, et al. Removal of Pb2+ ions from aqueous solutions using Posidonia oceanica collected from Tajora Beach (Libya). Int J Prog Sci Technol. 2021;25(2):595–601.
10. Allouche FN, et al. Pb(II) biosorption on Posidonia oceanica biomass. HAL Open Sci. 2024;7:13.
11. Tien C. Introduction to adsorption: basics, analysis, and applications. Amsterdam: Elsevier; 2019.
12. Anagnostopoulos VA, Manariotis ID, Karapanagioti HK, Chrysikopoulos CV. Removal of mercury from aqueous solutions by malt spent rootlets. Chem Eng J. 2012;213:135–141.
13. Dou B, Dupont V, Pan W, Chen B. Removal of aqueous toxic Hg(II) by synthesized TiO2 nanoparticles and TiO2/montmorillonite. Chem Eng J. 2011;166(2):631–638.
14. Hardani K, Buazar F, Ghanemi K, Kashisaz M, Baghlani-Nezhad M, Khaledi-Naseb A, et al. Removal of toxic mercury (II) from water via Fe3O4/hydroxyapatite nanoadsorbent: an efficient, economic and rapid approach. AASCIT J Nanosci. 2015;1(1):11–18.
15. Sharma A, Sharma A, Arya RK. Removal of mercury(II) from aqueous solution: a review of recent work. Sep Sci Technol. 2014;50(9):1310–1320.
16. Boulaiche W, Belhamdi B, Hamdi B, Trari M. Kinetic and equilibrium studies of biosorption of M (II)(M= Cu, Pb, Ni, Zn and Cd) onto seaweed Posidonia oceanica fibers. Appl Water Sci. 2019;9(8):173.
17. Mozurkewich M, Benson SW. Negative activation energies and curved Arrhenius plots. 1. Theory of reactions over potential wells. J Phys Chem. 1984;88(25):6429–6435.
18. Virga E, Spruijt E, de Vos WM, Biesheuvel PM. Wettability of amphoteric surfaces: the effect of pH and ionic strength on surface ionization and wetting. Langmuir. 2018;34(50):15174–15180.
19. Adewumi CN, Abvaghare ED, Emmanuel EJ. Kinetics–thermodynamics integration for improved understanding of adsorption mechanism: a critical perspective. World J Adv Res Rev. 2025;27(2):417–443.
20. Danat BT, et al. Review of adsorption isotherms models. Appl Water Sci. 2026;16:72.
21. Azizian S. Kinetic models of sorption: a theoretical analysis. J Colloid Interface Sci. 2004;276(1):47–52.

Received*: 10-06-2026 -* ***Accepted****: 08-08-2026 -* ***Published****: 17-08-2026*